



1 **Simulation of the evolution of biomass burning organic aerosol** 2 **with different volatility basis set schemes in PMCAMx-SRv1.0**

3
4 Georgia N. Theodoritsi^{1,2}, Giancarlo Ciarelli^{3,4}, Spyros N. Pandis^{1,2,3}

5 ¹*Department of Chemical Engineering, University of Patras, Patras, Greece*

6 ²*Institute of Chemical Engineering Sciences, Foundation for Research and Technology Hellas*
7 *(FORTH/ICE-HT), Patras, Greece*

8 ³*Department of Chemical Engineering, Carnegie Mellon University, Pittsburgh, USA*

9 ⁴*Now at: Institute for Atmospheric and Earth System Research/Physics, Faculty of Science,*
10 *University of Helsinki, Finland*

11 **Correspondence to: Spyros N. Pandis (spyros@chemeng.upatras.gr)*

12 13 **Abstract**

14 A source-resolved three-dimensional chemical transport model, PMCAMx-SR, was
15 applied in the continental U.S. to investigate the contribution of the various components (primary
16 and secondary) of biomass burning organic aerosol (bbOA) to organic aerosol levels. Two
17 different schemes based on the volatility basis set were used for the simulation of the bbOA
18 during different seasons. The first is the default scheme of PMCAMx-SR and the second is a
19 recently developed scheme based on laboratory experiments of the bbOA evolution.

20 The simulations with the alternative bbOA scheme predict much higher total bbOA
21 concentrations when compared with the base case ones. This is mainly due to the high emissions
22 of intermediate volatility organic compounds (IVOCs) assumed in the alternative scheme. The
23 oxidation of these compounds is predicted to be a significant source of secondary organic
24 aerosol. The impact of the other parameters that differ in the two schemes is low to negligible.
25 The monthly average maximum predicted concentrations of the alternative bbOA scheme were
26 approximately an order of magnitude higher than those of the default scheme during all seasons.

27 The performance of the two schemes was evaluated against observed total organic
28 aerosol concentrations from several measurement sites across the US. The results were mixed.
29 The default scheme performed better during July and September while the alternative scheme



30 performed a little better during April. These results illustrate the uncertainty of the corresponding
31 predictions, the need to quantify the emissions and reactions of IVOCs from specific biomass
32 sources, and to better constrain the total (primary and secondary) bbOA levels.

33

34 **1. Introduction**

35 Over the past decades, atmospheric aerosols, also known as particulate matter (PM), are
36 at the forefront of atmospheric chemistry research due to their adverse impacts on human health,
37 climate change, and visibility. More specifically, fine particulate matter with an aerodynamic
38 diameter less than 2.5 μm (PM_{2.5}) is associated with decreased lung function (Gauderman et al.,
39 2000), bronchitis incidents (Dockery et al., 1996), respiratory diseases (Pope, 1991; Schwartz et
40 al., 1996; Wang et al., 2008) and eventually increases in mortality (Dockery et al., 1993). PM_{2.5}
41 also affects the planet's energy balance (Schwartz et al., 1996), and causes visibility reduction in
42 urban centers but also rural areas (Seinfeld and Pandis, 2006).

43 One of the most important components of fine PM almost everywhere is organic aerosol
44 (OA) (Andreae and Crutzen, 1997; Roberts et al., 2001; Kanakidou et al., 2005). Despite its
45 importance, OA remains poorly understood due to its physicochemical complexity (Goldstein
46 and Galbally, 2007). OA is traditionally separated into primary (POA), which is emitted directly
47 into the atmosphere as particles, and secondary OA (SOA), which is OA that is formed from
48 gaseous precursors that after oxidation and condensation form organic particulate matter
49 (Seinfeld and Pandis, 2006). SOA includes components produced during the oxidation of semi-
50 volatile organic compounds (called SOA-sv), of intermediate-volatility organic compounds
51 (SOA-iv), and of volatile organic compounds (SOA-v). POA and SOA are further categorized
52 into anthropogenic (aPOA, aSOA) and biogenic (bPOA, bSOA) based on their sources.

53 Biomass burning is an important global source of OA (Puxbaum et al., 2007; Gelencser et
54 al., 2007) and other pollutants such as nitrogen oxides, carbon monoxide, and volatile organic
55 compounds. This source contributes around 75% of global combustion POA (Bond et al., 2004).
56 In this work, the term biomass burning includes wildfires in forests and other areas, prescribed
57 burning which is a small wildfire set intentionally (Tian et al., 2008; Chiodi et al., 2018) in order
58 to decrease the likelihood of major wildfires, agricultural waste burning, and residential burning.

59 The simulation of bbOA has been the topic of numerous studies all of them concluding
60 that it is an important source of fine particles (Tian et al., 2009). Most of them assumed that



61 bbOA is non-volatile and inert (Chung and Seinfeld, 2002; Kanakidou et al., 2005). Alvarado et
62 al. (2015) used the Aerosol Simulation Program that incorporates updates to the gas-phase
63 chemistry and SOA formation modules using observations from a biomass burning plume from a
64 prescribed fire in California. A method was presented for simultaneously accounting for the
65 impact of the unidentified intermediate volatility, semi-volatile, and extremely low volatility
66 organic compounds on the formation of OA, based on the volatility basis set (VBS) approach
67 (Robinson et al., 2007) for modeling OA and the concept of the mechanistic reactivity of a
68 mixture of organic compounds (Carter, 1994). Bergström et al. (2012) concluded that residential
69 wood combustion and wildfires are a major source of aerosol over large parts of Europe.
70 However, the simulated results are sensitive to the parameters used in the VBS framework.
71 Posner et al. (2019), using the standard version of PMCAMx, that incorporates the VBS scheme,
72 estimated that bbSOA from semivolatile and intermediate volatility organic compounds emitted
73 during biomass burning is one of the most important components of bbOA in the US.

74 Fountoukis et al. (2014) performed simulations in Europe using the PMCAMx model
75 during 2008-2009. The largest discrepancies of average PM₁ OA concentrations between model
76 and measurements were found during the winter. Ciarelli et al. (2017a, b) proposed an alternative
77 parameterization that was derived from biomass burning experiments conducted with emissions
78 from woodstoves, and was based on the volatility basis set (VBS) scheme (Koo et al., 2014).
79 This alternative parameterization was applied only to the residential heating sector. The
80 applicability of this parameterization to other biomass burning sources such as wildfires and
81 prescribed burning will be investigated in the present study. The alternative framework was
82 evaluated using CAMx for February – March 2009. The new scheme narrowed the difference
83 between predictions and observations compared to previous studies (Fountoukis et al., 2014), but
84 still underpredicted the observed SOA, whereas the bbPOA was generally overpredicted. The
85 same scheme was evaluated for 2011 in Europe using CAMx 6.3 (Jiang et al., 2019). The authors
86 concluded that the modified parameterization improved the model performance for total OA as
87 well as the OA components especially during the winter.

88 The aim of the current study is to implement the alternative VBS scheme proposed by
89 Ciarelli et al. (2017a, b) in the PMCAMx-SR model during different periods. These periods have
90 already been investigated by Theodoritsi et al. (2020) using the default PMCAMx-SR scheme.
91 That study concluded that during spring the PMCAMx-SR performance is good according to the



92 criteria proposed by Morris et al. (2005) but the model tends to underpredict the observed PM_{2.5}
93 OA. During the modeled summer period the PMCAMx-SR performance was average with a
94 tendency towards overprediction of the observed PM_{2.5} OA. Finally, during the fall the model
95 performance was average-to-problematic because the model overpredicted the OA levels. The
96 overprediction during this period was mainly due to the overprediction of the bbOA which is the
97 dominant OA source. We aim to further investigate whether the application of this new
98 parameterization that has improved bbOA predictions in Europe will close the gap between
99 predictions and observations in the US too.

100 In most modelling studies so far biomass burning OA (bbOA) is grouped with the rest of
101 the primary and secondary OA components and is simulated in exactly the same way. In this
102 study, PMCAMx-SR the three-dimensional chemical transport model (CTM) used simulates
103 bbOA components separately from the rest of the OA allowing the use of volatility distributions,
104 aging schemes, etc. that are specific to this source (Theodoritsi et al., 2019). At the same time,
105 this enhanced model (extension of PMCAMx) allows direct predictions of bbOA concentrations
106 since it tracks these species separately. Theodoritsi et al. (2020) used PMCAMx-SR to quantify
107 the importance of bbOA from prescribed burning activities in the US on air quality and human
108 health.

109 In the current study we will study in detail the impact of the different partitioning
110 parameters implemented in bbPOA description and bbSOA formation and evolution as proposed
111 by Ciarelli et al. (2017a, b). While the previous study of Theodoritsi et al. (2020) focused on the
112 role of prescribed burning as a source of bbOA, in this study all biomass burning sources are
113 grouped together.

114

115 **2. The chemical transport model PMCAMx-SR**

116 PMCAMx-SR is a source-resolved version of the three-dimensional CTM PMCAMx
117 (Murphy and Pandis, 2009; Tsimpidi et al., 2010; Karydis et al., 2010). The model simulates
118 emissions, advection, turbulent dispersion, removal by wet and dry deposition, chemistry in the
119 gas, aqueous and particulate phases and aerosol dynamics. Different gas-phase chemistry
120 mechanisms can be selected by the user. In this study the Carbon Bond 5 mechanism (Yarwood
121 et al., 2005; ENVIRON, 2015) is used expanded for the treatment of secondary organic aerosol
122 production. The extended version of the mechanism used simulates the concentrations of 103



123 gas-phase stable species and of 13 free radicals using 269 chemical reactions. The aerosol-size
124 composition distribution is simulated using the sectional method with eight size bins for the
125 diameter range from 40 nm to 10 μm and two more for larger sizes used for particles that have
126 grown to cloud droplets. The model simulates in total 67 aerosol components both inorganic and
127 organic

128 **2.1 Simulation of organic aerosol (base scheme)**

129 PMCAMx-SR uses the VBS framework (Donahue et al., 2006; Stanier et al., 2008) for
130 the simulation of the various components of OA. The VBS treats all primary and secondary OA
131 components as semi-volatile simulating their partitioning between the vapour and particle
132 phases. It also treats all of them as reactive allowing the simulation of both the initial stage of
133 formation of SOA but also later generations of reactions (often called “chemical aging”).
134 Volatility is expressed in the VBS using the effective saturation concentration at 298 K, C^* , and
135 the volatility distribution is split in logarithmically spaced volatility bins (differences of factors
136 of 10).

137 The emitted primary organic compounds include: volatile organic compounds (VOCs; C^*
138 $\geq 10^6 \mu\text{g m}^{-3}$), intermediate volatility organic compounds (IVOCs; C^* bins of 10^3 , 10^4 , 10^5 , and
139 $10^6 \mu\text{g m}^{-3}$), semi-volatile organic compounds (SVOCs; in the 1, 10, 100 $\mu\text{g m}^{-3}$ C^* bins) and
140 finally low volatility organic compounds (LVOCs; $C^* \leq 0.1 \mu\text{g m}^{-3}$) (Donahue et al., 2009).
141 PMCAMx-SR uses the generic POA volatility distribution proposed by Robinson et al. (2007) to
142 simulate the anthropogenic OA emissions from all sources except biomass burning. The total
143 VBS emissions are assumed to be 2.5 times the original non-volatile POA emissions in the
144 traditional inventory used for regulatory purposes. This default volatility distribution in previous
145 studies using PMCAMx was implemented to all sources of OA including biomass burning.

146 In PMCAMx-SR, the fresh and secondary bbOA components are modelled separately
147 from the other OA components. The gas-particle partitioning parameters used for bbPOA species
148 are the ones proposed by May et al. (2013). However, the volatility distribution proposed in that
149 study only includes compounds up to a volatility bin of $10^4 \mu\text{g m}^{-3}$. The total emissions of the
150 bbOA components in the $0.1\text{-}10^4 C^*$ bins are assumed to be equal to the non-volatile bbOA
151 emissions in the traditional inventory. Following the approach of Theodoritsi et al. (2020), the
152 total emissions of the more volatile IVOCs (C^* values of 10^5 to $10^6 \mu\text{g m}^{-3}$) are set equal to 0.5



153 times the original nonvolatile POA emissions. Therefore, the total biomass burning organic
154 emissions used in this study are 1.5 times the original POA emissions.

155 SOA from anthropogenic volatile organic compounds (aSOA-v) and SOA from biogenic
156 volatile organic compounds (bSOA-v) are represented by four volatility bins with C^* values
157 ranging from 1 to $10^3 \mu\text{g m}^{-3}$ at 298 K. Long-range transport OA is assumed to be heavily
158 oxidized OA and is treated in PMCAMx-SR as nonvolatile and nonreactive. Overall, the OA
159 components included explicitly in PMCAMx-SR are: fresh primary anthropogenic OA (POA),
160 fresh primary bbOA (bbPOA), anthropogenic SOA from VOCs (aSOA), biogenic SOA (bSOA),
161 SOA from semi-volatile anthropogenic organic compounds (SOA-sv), SOA from intermediate-
162 volatility anthropogenic organic compounds (SOA-iv), bbSOA from semi-volatile organic
163 compounds (bbSOA-sv), bbSOA from intermediate-volatility organic compounds (bbSOA-iv),
164 and long-range transport OA.

165 All OA components (except from long range transport OA) are treated as chemically
166 reactive in PMCAMx-SR. The rate constant used for the chemical aging reactions with the OH
167 radical is the same as the one currently used for all primary organic vapors in the VBS and has a
168 value of $4 \times 10^{-11} \text{ cm}^3 \text{ molec}^{-1} \text{ s}^{-1}$. SOA-sv, SOA-iv, bbSOA-sv and bbSOA-iv components are
169 assumed to further react with OH radicals in the gas phase, resulting in the formation of lower-
170 volatility SOA and bbSOA components. Semi-volatile aSOA components are assumed to react
171 with OH in the gas phase with a rate constant of $1 \times 10^{-11} \text{ cm}^3 \text{ molec}^{-1} \text{ s}^{-1}$ (Atkinson and Arey,
172 2003). Chemical aging of bSOA is assumed to lead to a small net change of mass and is
173 neglected (Murphy and Pandis, 2010). All the aging reactions mentioned above are assumed to
174 reduce the volatility of the reacted vapor by one order of magnitude. These reactions are assumed
175 to result in an increase of the OA mass by 7.5% due to the added oxygen.

176 Table 1 summarizes the VBS parameters of all OA species in the base simulation. All
177 POA and bbPOA components are assumed to have an average molecular weight of 250 g mol^{-1} ,
178 aSOA components of 150 g mol^{-1} , while bSOA species of 180 g mol^{-1} . The effective enthalpies
179 of vaporization of both POA and bbPOA species are based on fits of diesel and wood-smoke
180 partitioning data (Lipsky and Robinson, 2006; Shrivastava et al., 2006).

181

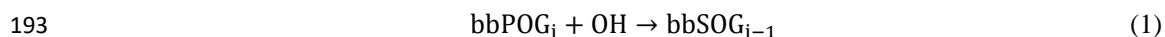
182

183



184 2.2 Alternative bbOA scheme

185 The scheme of Ciarelli et al. (2017a, b) for the simulation of the emissions of organics
186 from residential heating biomass burning and their evolution in the atmosphere during winter
187 was also implemented in PMCAMx-SR. The organic PM emissions (assumed nonvolatile in the
188 original inventory) are distributed in this scheme across five volatility bins with saturation
189 concentrations values ranging from 10^{-1} and $10^3 \mu\text{g m}^{-3}$ following the volatility distribution and
190 enthalpy of vaporization proposed by May et al. (2013). Organic vapors in this volatility range
191 are assumed to react with OH forming semi-volatile oxidation products with an order of
192 magnitude lower volatility:



194 where i is the corresponding volatility bin, bbPOG_i is the primary emissions in the gas phase and
195 bbSOG_i are their oxidation products. Fragmentation processes are implicitly assumed to balance
196 the effect of the increase in oxygen content of the reacting molecules.

197 All emitted IVOCs in this bbOA scheme are assumed to have a C^* value of $10^6 \mu\text{g m}^{-3}$
198 which is at the high end of the IVOC saturation concentration range. The emission rate of these
199 IVOCs is assumed to be 4.75 times the primary OA emissions in the original inventory. The
200 IVOCs are assumed to react according to the following reaction:



203 yielding secondary products with saturation concentration ranging from $C^*=1$ to $10^3 \mu\text{g m}^{-3}$. In
204 this reaction bbPOG_{10^6} stands for the primary emissions in the volatility bin with C^* value equal
205 to $10^6 \mu\text{g m}^{-3}$, whereas bbSOG_{10^3} to bbSOG_{10^0} are the secondary gas phase oxidation products of
206 the IVOCs with C^* values ranging from 10^3 to $10^0 \mu\text{g m}^{-3}$. For both primary and secondary
207 compounds aging is simulated assuming a gas phase reaction rate constant with OH of 4×10^{-11}
208 $\text{cm}^3 \text{molec}^{-1} \text{s}^{-1}$. The lowest volatility secondary bbOA components in this scheme have $C^*=10^{-1}$
209 $\mu\text{g m}^{-3}$ since the $C^*=1 \mu\text{g m}^{-3}$ species can react with OH to form lower volatility products.

210 Table 1 also summarizes the volatility distribution, the molecular weights, and enthalpies
211 of vaporization of all bbOA species used in the alternative bbOA modeling scheme used in this
212 study. The enthalpies of vaporization used in this bbOA scheme are the ones proposed in Ciarelli
213 et al. (2017a, b).

214



215 3. Model application

216 In this study PMCAMx-SR is used to simulate three seasonally representative months
217 (April, July, and September) during 2008 for the continental US. The modeling domain also
218 included southern Canada and northern Mexico. The first two days of each simulation were
219 excluded from our analysis to allow for model spin-up, but the corresponding results are shown
220 in time series plots. The modeling domain covers a region of 5328×4032 km² with 36×36 km
221 grid cell resolution and 25 vertical layers extending up to 19 km (Figure 1). An annual CAMx
222 simulation was performed for the same domain to obtain the necessary initial conditions used in
223 our simulations for each month (ENVIRON, 2013).

224 The Weather Research and Forecast Model (WRF) version 3.3.1 (NCAR, 2012) was used
225 to produce the meteorological inputs needed by PMCAMx-SR. The land-use data were based on
226 the U.S. Geological Survey Geographic Information Retrieval and Analysis System (USGS
227 GIRAS) database. The photolysis rate input data were produced by the NCAR Tropospheric
228 Ultraviolet and Visible (TUV) radiation model. The chemical boundary conditions were based
229 on simulations using the MOZART global CTM (Emmons et al., 2010). Additional details about
230 the model inputs can be found in Posner et al. (2019) and Theodoritsi et al. (2020).

231 The emission inventory used in the current study tracks separately the biomass burning
232 emissions from the emissions of other sources. The latter are based on the U.S. National
233 Emissions Inventory (2008 NEI). Biomass burning emissions include emissions of prescribed
234 burning, agricultural burning, and wildfires and the methods used for their estimation inventory
235 be found in WRAP (2013; 2014). The fire activity data used are described in Ruminski et al.
236 (2006), Eidenshink et al. (2007) and Mavko and Randall (2008). The approach used for the
237 preparation, processing, and validation of fire activity data were similar to those of Wiedinmyer
238 et al. (2006) and Raffuse et al. (2009). For fire consumption estimates CONSUME3 (Joint Fire
239 Science Program, 2009) was used for all biomass burning sources except agricultural burns for
240 which the method from the WRAP 2002 emissions inventory was employed (WRAP, 2005).

241 During all three examined periods biomass burning was a significant OA source mainly
242 in the Southeast U.S. (Posner et al., 2019; Theodoritsi et al., 2020). Specifically, during April,
243 July and September respectively this source represents approximately 25%, 65% and 37% of the
244 total OA emissions. During April 19% of the domain-averaged bbOA emissions rate are due to
245 agricultural burning, 47% to prescribed burning, and 34% to wildfires. During July, due to the



246 very high wildfire emissions mainly in northern California, the domain-averaged bbOA
247 emissions are mostly (96%) due to this source. Agricultural burning contributed 1% and
248 prescribed burning the remaining 3%. For September, wildfires in the west were still the
249 dominant source and they were responsible for 73% of the domain bbOA emissions. Prescribed
250 burning was a significant source (22% of the bbOA emission), while agricultural burning was
251 responsible for 5% of the emissions. Posner et al. (2019) and Theodoritsi et al. (2020) have
252 presented analysis of the spatial distribution and magnitude of these bbOA emissions.

253

254 **4. Predicted bbOA concentrations**

255 In this section the predictions of PMCAMx-SR for the base case and the alternative
256 bbOA scheme are analyzed. In this work bbOA is defined as the sum of primary (bbPOA) and
257 secondary (bbSOA) OA. The latter is the sum of bbSOA originating from semi-volatile organic
258 compounds (bbSOA-sv) and from IVOCs (bbSOA-iv). The small SOA contribution from VOCs
259 (Posner et al., 2019) is not explicitly accounted in the bbSOA, but is included in the aSOA and
260 bSOA simulated by the model. The results of the PMCAMx-SR simulations with the two
261 schemes are shown in Figures 1-3.

262 During April both schemes predict approximately the same bbPOA concentrations
263 (Figure 1) that were as high as $3.5 \mu\text{g m}^{-3}$ on a monthly average basis in the southeastern US.
264 These high levels were mainly due to prescribed burning. The differences in predicted bbPOA
265 levels by the two models were less than $0.1 \mu\text{g m}^{-3}$ (Figure 4) something expected given that they
266 use the same volatility distributions for the primary LVOCs and SVOCs. Predicted average
267 ground bbPOA levels over the US were approximately $0.02 \mu\text{g m}^{-3}$. The predicted bbSOA-sv
268 concentration fields were also quite similar (differences less than $0.1 \mu\text{g m}^{-3}$) for the two schemes
269 (Figure 1). This is also the consequence of the similarity of the volatility distributions and
270 chemical aging parameterizations used by the two schemes in the SVOC volatility range of the
271 biomass burning emissions. While the average bbSOA-sv levels over the domain were quite
272 similar to those of the bbPOA (around $0.02 \mu\text{g m}^{-3}$), the peak levels were lower with a maximum
273 monthly average concentration of $0.5 \mu\text{g m}^{-3}$. This spreading of the bbSOA-sv further from the
274 fires is the result of the time needed for the corresponding reactions to take place. The
275 predictions of the two schemes are quite different though for bbSOA-iv (Figure 1). For the base
276 scheme, the bbSOA-iv is equally important as the bbPOA and the bbSOA-iv contributes on



277 average $0.02 \mu\text{g m}^{-3}$ of OA over the domain. The peak monthly average bbSOA-iv concentration
278 is predicted to be approximately $0.2 \mu\text{g m}^{-3}$ in the southeast. The predictions for bbSOA-iv for
279 the alternative scheme are approximately an order of magnitude higher, with a maximum average
280 of $2 \mu\text{g m}^{-3}$ and a domain average of $0.2 \mu\text{g m}^{-3}$ (Figure 1). Even if the IVOC emissions are
281 assumed to be more volatile in the alternative scheme, their high emission rate allows the
282 production of significant concentrations of secondary OA from biomass burning that extend over
283 the eastern half of the country during this photochemically active period.

284 Both models predict that during April the bbSOA is the dominant component of bbOA on
285 average over the domain and even if it peaks in South Carolina with high levels in North
286 Carolina and Georgia, it has average concentrations above $0.1 \mu\text{g m}^{-3}$ in most areas of the
287 Eastern US (Figure 5a). The alternative scheme predicts that this bbSOA contribution is a factor
288 of 5-10 higher and around or above $1 \mu\text{g m}^{-3}$ in the Eastern US. Adding everything together the
289 alternative scheme predicts an average bbOA concentration of $0.3 \mu\text{g m}^{-3}$ that is a factor of 5
290 higher than the average predicted by the base scheme (Figure 6a).

291 During July, several major wildfires occurred in California and consequently bbOA
292 levels were particularly high in the western US (Figure 2a) reaching levels around $100 \mu\text{g m}^{-3}$.
293 This presents a very different situation compared to the spring month discussed above. Once
294 more, the predictions of the two schemes for bbPOA were quite similar (differences less than
295 20%), even if the concentration levels at least in California were much higher. Despite the
296 intensity of the fires in California, the low emissions in the rest of the country resulted in similar
297 average bbPOA levels over the domain as in April ($0.15 \mu\text{g m}^{-3}$) for both schemes. Both schemes
298 predicted similarly high bbSOA-sv levels with monthly average values up to $15 \mu\text{g m}^{-3}$ and
299 domain average values of $0.2 \mu\text{g m}^{-3}$ (Figure 2b). The alternative aging scheme predicts high
300 bbSOA-iv that dominate the overall bbOA in the domain with an average of $2 \mu\text{g m}^{-3}$. The
301 average bbSOA-iv but also the peak levels predicted by the base scheme are more than an order
302 of magnitude lower (Figure 2c). The average bbSOA predicted by the base scheme was
303 approximately a factor of 7 lower (0.3 versus $2 \mu\text{g m}^{-3}$) for the domain (Figure 5), while the total
304 bbOA was a factor of 5 lower (Figure 6). The differences between the two schemes exceeded 10
305 $\mu\text{g m}^{-3}$ on a monthly average basis over California, and were above $1 \mu\text{g m}^{-3}$ over a large part of
306 the western US (Figure S1).



307 During September there were major wild fires once more in California but also in Oregon
308 (Figure 3). Smaller fires were present in New Mexico and in several southeastern states. The
309 predicted bbPOA average concentration, similar for both schemes, were the lowest of the three
310 simulated periods with a value of approximately $0.1 \mu\text{g m}^{-3}$. The local monthly maxima were 65
311 and $75 \mu\text{g m}^{-3}$ for the base case and the alternative aging scheme respectively (Figure 3a). The
312 average bbSOA-sv concentration based on the predictions of both schemes were a factor of 6
313 higher (around $0.6 \mu\text{g m}^{-3}$) than the average bbPOA concentration. The average bbSOA-sv
314 during the month exceeded $0.1 \mu\text{g m}^{-3}$ over a wide region covering most of the western coast of
315 the US and parts of the Pacific. The peak monthly average bbSOA-sv concentration was $7 \mu\text{g m}^{-3}$
316 for both simulations. Finally, for the bbSOA-iv the alternative scheme predicted both domain
317 average and peak concentrations that were approximately an order of magnitude higher than the
318 base scheme (Figure 3c). For the base case simulation, bbSOA-iv was as high as $4 \mu\text{g m}^{-3}$ with a
319 monthly average value of approximately $0.05 \mu\text{g m}^{-3}$ whereas the same values for the alternative
320 aging scheme were $45 \mu\text{g m}^{-3}$ and $0.7 \mu\text{g m}^{-3}$ respectively. As a result, the alternative scheme
321 predicts average bbSOA levels that are a factor of 7 higher than the base case (0.1 versus $0.7 \mu\text{g m}^{-3}$)
322 (m^{-3}) (Figure 5c) and total bbOA levels that are a factor of 4 higher (Figure 6c). For the peak
323 monthly average concentrations, the differences are a factor of 5 for bbSOA and a factor of 1.5
324 for bbOA (given that the bbPOA is a dominant component near the fires).

325

326 **5. Importance of the VBS parameters used in the two bbOA schemes**

327 The difference in the IVOC emissions and aging schemes appears to explain a large
328 fraction of the differences in the predictions of the two schemes in the simulated periods.
329 However, there are other potentially important differences in the parameters used in the two
330 schemes. These different parameters include the enthalpy of vaporization and the molecular
331 weights of the various bbOA components. The effect of these together with the effect of the
332 assumed volatility distributions of the emitted bbOA components and the assumed aging
333 schemes was investigated. Sensitivity tests were performed for one of the three periods (April
334 2008) to quantify the individual effect of these parameters on the predictions of PMCAMx-SR.
335 The results of these tests and their comparison with the base case results are analyzed in the
336 subsequent sections.

337



338 **5.1 Enthalpy of vaporization**

339 In this first sensitivity test, we changed the effective enthalpies of vaporization of the
340 bbOA components (bbPOA, bbSOA-sv, bbSOA-iv) in the base scheme from their original values
341 that varied from 64 to 106 kJ mol⁻¹ to those of the alternative scheme (Table 1). The new values
342 were equal to 35 kJ mol⁻¹ for the bbSOA components and varied from 37 to 70 kJ mol⁻¹ for the
343 bbPOA. This test allows us to quantify the importance of the significantly lower enthalpies used
344 in the alternative scheme based on the work of Ciarelli et al. (2017a, b). All other parameters of
345 the base scheme were kept the same.

346 The changes in the predictions of the model were small, a few percent or less (Figure S2).
347 The use of the higher original enthalpies of vaporization resulted in a little higher concentration
348 for all bbOA components. The maximum monthly average changes were 0.3 µg m⁻³ for bbPOA,
349 0.03 µg m⁻³ for bbPOA-sv, 0.03 µg m⁻³ bbSOA-iv and 0.4 µg m⁻³ for total bbOA all near
350 Savannah, Georgia. However, for most of the US the change in total bbOA was less than 0.05 µg
351 m⁻³. Therefore, the major differences in bbSOA-iv predictions of the base and alternative scheme
352 were not due to their different enthalpies of vaporization.

353

354 **5.2 Molecular weights**

355 The base scheme assumes a molecular weight of 250 g mol⁻¹ for all bbOA components
356 while a range of molecular weights from 113 to 216 g mol⁻¹ are used in the alternative scheme
357 (Table 1). These variable molecular weights are also intended to account for fragmentation
358 effects and are accompanied by a stoichiometric coefficient equal to unity (instead of 1.075 in
359 the base scheme). We replaced the molecular weights of the base scheme with those of the
360 alternative, changed the stoichiometric coefficients in the aging reactions from 1.075 to 1, kept
361 everything else the same, and repeated the April simulation.

362 The impact of these changes in the molecular weight values and stoichiometric
363 coefficients was small (Figure 7). The maximum concentration changes for the monthly average
364 concentrations were 0.02 µg m⁻³ for bbPOA, 0.03 µg m⁻³ for bbSOA-sv, 0.1 µg m⁻³ for bbPOA-iv
365 and 0.1 µg m⁻³ for total bbOA all in the borders between South Carolina and Georgia. The use of
366 the Ciarelli et al. (2017) parameters (molecular weights and aging stoichiometric coefficients)
367 led to very small reductions of the bbPOA and bbSOA-sv levels and small increases in the
368 bbSOA-iv levels. The latter dominated the overall bbOA change which increased by 0.01 to 0.03



369 $\mu\text{g m}^{-3}$ in large parts of the Eastern US and by 0.03-0.1 $\mu\text{g m}^{-3}$ in South Carolina and Georgia.
370 These changes are still only a few percent. This small impact of the changes is partially due to
371 the fact that they cancel each other to a large extent. The decrease in molecular weights leads to
372 increased partitioning towards the particle phase and therefore higher bbOA levels, where the
373 decrease in the aging stoichiometric coefficients has the opposite effect for the secondary
374 components.

375

376 **5.3 Volatility distribution of biomass burning emissions**

377 In this test, the emissions of the various organic compounds in the VBS from biomass
378 burning were changed from these of the base scheme to those of Ciarelli et al. (2017) (Table 1).
379 This change does not affect the LVOC emissions and the SVOC emissions for C* less or equal
380 than $10^2 \mu\text{g m}^{-3}$. However, it increases the emissions of the $10^3 \mu\text{g m}^{-3}$ volatility bin (by adding to
381 these emissions those that are in the $10^4 \mu\text{g m}^{-3}$ bin) and also increases significantly the
382 emissions of the IVOCs in the $10^6 \mu\text{g m}^{-3}$ while it zeros those in the $10^5 \mu\text{g m}^{-3}$ bin.

383 The use of the Ciarelli et al. (2017) volatility distributions leads to significant changes of
384 the predicted bbOA concentration levels (Figure 8). In all areas, and for all bbOA components it
385 predicts higher concentrations. The maximum concentration differences between the two
386 simulations were $0.1 \mu\text{g m}^{-3}$ for bbPOA, $0.1 \mu\text{g m}^{-3}$ for bbSOA-sv and $1.5 \mu\text{g m}^{-3}$ for bbSOA-iv.
387 These differences are quite similar in magnitude to those of the base and alternative schemes
388 (Figure 4a). This strongly suggests that the differences in the assumed bbOA volatility-resolved
389 emissions is mainly responsible for the differences in the bbOA predictions of the two schemes.
390 For example, for the average total bbOA in the modeling domain the change in the volatility
391 distributions led to an increase of the base case results by $0.14 \mu\text{g m}^{-3}$. This should be compared
392 with the $0.2 \mu\text{g m}^{-3}$ that is the difference between the average bbOA predicted by the base and
393 alternative schemes.

394 The most important difference is the change in the IVOC emissions resulting in
395 significant changes of the bbSOA-iv. The predicted bbSOA-iv of PMCAMx-SR with the base
396 scheme using the default and the Ciarelli et al. (2017) bbOA volatility distributions are depicted
397 in Figure 9. The monthly maximum concentration was predicted to be 0.2 and $1.5 \mu\text{m m}^{-3}$ for the
398 base case and the alternative bbOA scheme respectively in South Carolina. This is also



399 consistent, with our conclusion that the difference in the IVOC emissions is the leading cause of
400 the differences of the predictions of the base and alternative schemes.

401

402 **6. Model evaluation with field measurements**

403 The predictions of PMCAMx-SR for daily average PM_{2.5} were compared to the
404 corresponding measurements in 161 STN sites (located mainly in urban areas) and 162
405 IMPROVE sites (located mostly in rural and remote areas). These measurements were collected
406 once every three days. Given that most measurements were collected in periods during which the
407 corresponding site was not impacted by biomass burning, the use of the complete data set would
408 complicate the interpretation of the evaluation results. To avoid this complication, we have
409 followed Posner et al. (2019) and selected only the periods during which the base case of
410 PMCAMx-SR predicts daily average concentrations higher than a threshold value. Three such
411 thresholds were used to denote all periods with even a low biomass burning impact (threshold
412 0.1 µg m⁻³), all periods with intermediate or higher impact (threshold 0.5 µg m⁻³) and periods
413 with high impact (threshold 1 µg m⁻³).

414 The statistical metrics that were used for the evaluation of the two schemes are the mean
415 bias (MB), the mean absolute gross error (MAGE), the fractional bias (FBIAS), and the
416 fractional error (FERROR) (Fountoukis et al., 2011):

$$417 \quad MB = \frac{1}{n} \sum_{i=1}^n (P_i - O_i) \quad (3)$$

$$418 \quad MAGE = \frac{1}{n} \sum_{i=1}^n |P_i - O_i| \quad (4)$$

$$419 \quad FBIAS = \frac{2}{n} \sum_{i=1}^n \frac{(P_i - O_i)}{(P_i + O_i)} \quad (5)$$

$$420 \quad FERROR = \frac{2}{n} \sum_{i=1}^n \frac{|P_i - O_i|}{(P_i + O_i)} \quad (6)$$

421 where P_i is the predicted value of the pollutant concentration, O_i is the corresponding observed
422 value and n is the total number of data points used for the comparison.

423 Theodoritsi et al. (2020) have already analyzed the performance of the base scheme of
424 PMCAMx-SR for the same three periods. They concluded that during April the performance of
425 the base scheme is good according to the Morris et al. (2005) criteria and the model tends to
426 underpredict OA (fractional bias -0.16, fractional error 0.51 for the low threshold). PMCAMx-
427 SR showed little bias (3-6%) during July but had a relatively high fractional error (around 55%),



428 so its summer performance was considered average for the periods affected by biomass burning.
429 Finally, the model overpredicted the OA levels in September with the errors increasing when the
430 predicted bbOA concentration increased. This made its performance average to problematic
431 during this period. The metrics of this evaluation by Theodoritsi et al. (2020) for the base case
432 PMCAMx-SR simulation can also be found in Table S1 for completeness.

433 The bbOA predictions of the alternative scheme are in general higher than those of the
434 base scheme. This leads to a small improvement of the performance of PMCAMx-SR during
435 April especially for the low bbOA threshold (Table 2). The model now tends to overpredict OA,
436 while the base scheme underpredicted. For this case, the fractional bias is reduced (in absolute
437 terms) from -0.16 to 0.11 and the fractional error from 0.51 to 0.48. The improvements are minor
438 for the medium threshold, while for the high threshold the fractional bias increases (from -0.14 to
439 0.28) while the fractional error decreases (from 0.53 to 0.5). So overall, the use of the alternative
440 scheme appears to lead to a small improvement of the PMCAMx-SR predictions during this
441 period, but with a tendency towards overprediction especially close to the sources of biomass
442 burning.

443 During July, the base scheme reproduced the OA observations in areas affected by
444 biomass burning with little bias. The alternative scheme predicts a significantly higher SOA-iv
445 production during this period and results in a substantial overprediction of the OA levels in areas
446 with bbOA above all three thresholds (Table 2). The bias increases for the areas closer to the
447 fires (higher threshold). These results strongly suggest that the alternative scheme is too
448 aggressive in the production of SOA-iv during this summertime period with intensive wild fires.

449 PMCAMx-SR using the base scheme has difficulties reproducing the OA concentrations
450 in areas affected by fires. Given that the base scheme already overpredicts OA levels, the
451 increased SOA-iv predicted by the alternative scheme leads to additional deterioration of the
452 model performance. The alternative scheme substantially overpredicts OA and the fractional bias
453 increases closer to the sources of biomass burning. Overall, the performance of the alternative
454 scheme during September is like that during July.

455

456 7. Conclusions

457 An alternative bbOA scheme based on the work of Ciarelli et al. (2017a, b) has been used
458 in PMCAMx-SR to quantify the impact of bbOA on ambient particulate matter levels across the



459 continental U.S during April, July and September 2008. The alternative parameterization was
460 originally developed based on residential heating biomass burning experiments (i.e. combustion
461 in stoves). In this study we test its applicability for the simulation of the bbOA from other
462 sources (wildfires, prescribed and agricultural burning) in different periods.

463 The alternative scheme predicts in general much higher bbOA levels than the baseline
464 scheme for all seasons. Both schemes suggest that secondary production is a major process for
465 the average bbOA levels over the US in all examined periods. However, the alternative scheme
466 predicts that the production of secondary aerosol from intermediate volatility organic compounds
467 emitted during biomass burning is a factor of 5-10 higher than that of the base scheme. The
468 differences in the predictions of the other bbOA components (primary bbOA and bbOA from
469 semivolatile compounds) are low to modest.

470 A set of sensitivity tests showed that the most important difference between the two
471 schemes is the assumed emission rate of intermediate volatility organic compounds together with
472 their oxidation to form secondary organic aerosol. The impact of other different parameters,
473 including the assumed enthalpies of vaporization and molecular weights was small.

474 The performance of PMCAMx-SR using the two schemes was evaluated against
475 observed values obtained from 161 STN and 162 IMPROVE network measurement sites across
476 the US. During April the use of the alternative scheme leads to a small improvement of the
477 performance of PMCAMx-SR. However, during the more photochemically active periods of July
478 and September, with intense wild fires the PMCAMx-SR performance for OA deteriorates when
479 the alternative scheme is used instead of the base scheme. This strongly suggests that the
480 production of SOA-iv under these conditions is too aggressive. Fragmentation reactions may
481 become more important under these conditions leading to lower production of secondary organic
482 aerosol Our analysis suggests that the alternative scheme could be used during the spring-like
483 conditions, but it should probably be avoided during summer-like periods characterized by
484 intensive wild-fires activities.

485

486 *Code availability:* The PMCAMx-SRv1.0 code is available in Zenodo in <https://doi.org/10.5281/zenodo.4071362>.

488 *Data availability:* The data in the study are available from the authors upon request
489 (spyros@chemeng.upatras.gr).



490 *Author contributions:* GNT wrote the code, conducted the simulations, analysed the results, and
491 wrote the paper. GC contributed to the design of the code, analysis of the results, and the writing
492 of the paper. SNP was responsible for the design of the study, the synthesis of the results and
493 contributed to the writing of the paper.

494 *Competing interests.* The authors declare that they have no conflict of interest.

495 *Acknowledgement:* This work has received funding from the European Union's Horizon 2020
496 research and innovation programme under project FORCeS, grant agreement No 821205.

497

498 **References**

499 Alvarado, M. J., Lonsdale, C. R., Yokelson, R. J., Akagi, S. K., Coe, H., Craven, J. S., Fischer,
500 E. V., McMeeking, G. R., Seinfeld, J. H., Soni, T., Taylor, J. W., Weise, D. R., and
501 Wold, C. E.: Investigating the links between ozone and organic aerosol chemistry in a
502 biomass burning plume from a prescribed fire in California chaparral, *Atmos. Chem.*
503 *Phys.*, 15, 6667–6688, 2015.

504 Andreae, M. O. and Crutzen, P. J.: Atmospheric aerosols: biogeochemical sources and role in
505 atmospheric chemistry, *Science*, 276, 1052–1058, 1997.

506 Atkinson, R. and Arey, J.: Atmospheric degradation of volatile organic compounds, *Chem. Rev.*,
507 103, 4605–4638, 2003.

508 Bergström, R., Denier van der Gon, H. A. C., Prévôt, A. S. H., Yttri, K. E., and Simpson, D.:
509 Modelling of organic aerosols over Europe (2002–2007) using a volatility basis set
510 (VBS) framework: application of different assumptions regarding the formation of
511 secondary organic aerosol, *Atmos. Chem. Phys.*, 12, 8499–8527, 2012.

512 Bond, T. C., Streets, D. G., Yarber, K. F., Nelson, S. M., Woo, J. H., and Klimont, Z.: A
513 technology-based global inventory of black and organic carbon emissions from
514 combustion, *J. Geophys. Res.*, 109, D14203, doi: 10.1029/2003 JD003697, 2004.

515 Chiodi, A.M., Larkin, N.S., and Varner, J.M., An analysis of Southeastern US prescribed burn
516 weather windows: seasonal variability and El Nino associations, *International Journal of*
517 *Wildland Fire*, 27, 176–89, 2018.

518 Chung, S. H. and J. H. Seinfeld J. H.: Global distribution and climate forcing of carbonaceous
519 aerosols, *J. Geophys. Res.*, 107, 4407, doi:10.1029/2001 JD001397, 2002.



- 520 Ciarelli, G., Aksoyoglu, S., El Haddad, I., Bruns, E.A., Crippa, M., Poulain, L., Äijälä, M.,
521 Carbone, S., Freney, E., O'Dowd, C., Baltensperger, U., and Prévôt, A.S.H.: Modelling
522 winter organic aerosol at the European scale with CAMx: evaluation and source
523 apportionment with a VBS parameterization based on novel wood burning smog chamber
524 experiments, *Atmos. Chem. Phys.*, 17, 7653–7669, 2017a.
- 525 Ciarelli, G., El Haddad, I., Bruns, E., Aksoyoglu, S., Möhler, O., Baltensperger, U., and Prévôt,
526 A.S.H.: Constraining a hybrid volatility basis-set model for aging of wood-burning
527 emissions using smog chamber experiments: a box-model study based on the VBS
528 scheme of the CAMx model (v5.40), *Geosci. Model Dev.* 10, 2303–2320, 2017b.
- 529 Dockery, W. D., Pope, C. A., Xu, X., Spengler, J. D., Ware, J. H., Fay Jr., M. E., Ferris, B. G.,
530 and Speizer, F. E.: An association between air pollution and mortality in six U.S. cities,
531 *New Engl. J. Med.*, 329, 1753–1759, 1993.
- 532 Dockery, D. W., Cunningham J., Damokosh A. I., Neas L. M., Spengler J. D., Koutrakis P.,
533 Ware J. H., Raizenne M., and Speizer F. E.: Health effects of acid aerosols on North
534 America children: Respiratory symptoms, *Environ. Health Persp.*, 104, 26821–26832,
535 1996.
- 536 Donahue, N. M., Robinson, A. L., Stanier, C. O., and Pandis, S. N.: Coupled partitioning,
537 dilution, and chemical aging of semivolatile organics, *Environ. Sci. Technol.*, 40, 2635–
538 2643, 2006.
- 539 Donahue, N.M., Robinson, A.L., and Pandis, S.N.: Atmospheric organic particulate matter: from
540 smoke to secondary organic aerosol, *Atmos. Environ.*, 43, 94-106, 2009.
- 541 Eidenshink, J., Schwind, B., Brewer, K., Zhu, Z., Quayle, B., and Howard, S.: A project for
542 monitoring trends in burn severity, *Fire Ecology*, 3, 3–21, 2007.
- 543 Emmons, L.K., Walter, S., Hess, P.G., Lamarque, J.-F., Pfister, G.G., Fillmore, D., Granier, C.,
544 Guenther, A., Kinnison, D., Laepple, T., Orlando, J., Tie, X., Tyndall, G., Wiedinmyer,
545 C., Baughcum, S.L., and Kloster, S.: Description and evaluation of the Model for Ozone
546 and Related Chemical Tracers, version 4 (MOZART-4), *Geosci. Model Dev.*, 3, 43-67,
547 2010.
- 548 ENVIRON: Western Regional Air Partnership (WRAP) west-side jump start air quality
549 modeling study (WestJumpAQMS) final modeling protocol. Prepared by ENVIRON
550 International Corporation, Novato, California, 2013.



- 551 ENVIRON: User's guide to the comprehensive air quality model with extensions (CAMx),
552 version 6.2. Prepared by ENVIRON International Corporation, Novato, California, 2015.
- 553 Fountoukis, C., Racherla, P.N., Denier van der Gon, H.A. C., Polymeneas, P., Charalampidis,
554 P.E., Pilinis, C., Wiedensohler, A., Dall'Osto, M., O'Dowd, C., and Pandis, S.N.:
555 Evaluation of a three-dimensional chemical transport model (PMCAMx) in the European
556 domain during the EUCAARI May 2008 campaign, *Atmos. Chem. Phys.*, 11, 10331–
557 10347, 2011.
- 558 Fountoukis, C., Butler, T., Lawrence, M. G., Denier van der Gon, H. A. C., Visschedijk, A. J. H.,
559 Charalampidis, P., Pilinis, C., and Pandis, S. N.: Impacts of controlling biomass burning
560 emissions on wintertime carbonaceous aerosol in Europe, *Atmos. Environ.*, 87, 175–182,
561 2014.
- 562 Gauderman, W. J., McConnel R., Gilliland F., London S., Thomas D., Avol E., Vora H.,
563 Berhane K., Rappaport E. B., Lurmann F., Margolis H. G., and Peters J.: Association
564 between air pollution and lung function growth in southern California children, *Am. J.*
565 *Resp. Crit. Care*, 162, 1383–1390, 2000.
- 566 Gelencser, A., May, B., Simpson, D., Sanchez-Ochoa, A., Kasper-Giebl, A., Puxbaum, H.,
567 Caseiro, A., Pio, C., and Legrand, M.: Source apportionment of PM_{2.5} organic aerosol
568 over Europe: primary/secondary, natural/anthropogenic, and fossil/biogenic origin, *J.*
569 *Geophys. Res.*, 112, D23S04, doi:10.1029/2006JD008094, 2007.
- 570 Goldstein, A. H., and Galbally, I. E.: Known and unexplored organic constituents in the earth's
571 atmosphere, *Environ. Sci. Technol.*, 41, 1514– 1521, 2007.
- 572 Jiang, J., Aksoyoglu, S., El-Haddad, I., Ciarelli, G., Denier van der Gon, H. A. C., Canonaco, F.,
573 Gilardoni, S., Paglione, M., Minguillón, M. C., Favez, O., Zhang, Y., Marchand, N., Hao,
574 L., Virtanen, A., Florou, K., O'Dowd, C., Ovadnevaite, J., Baltensperger, U., and Prévôt,
575 A. S. H.: Sources of organic aerosols in Europe: a modeling study using CAMx with
576 modified volatility basis set scheme, *Atmos. Chem. Phys.*, 19, 15247–15270, 2019.
- 577 Kanakidou, M., Seinfeld, J. H., Pandis, S. N., Barnes, I., Dentener, F. J., Facchini, M. C., Van
578 Dingenen, R., Ervens, B., Nenes, A., Nielsen, C. J., Swietlicki, E., Putaud, J. P.,
579 Balkanski, Y., Fuzzi, S., Horth, J., Moortgat, G. K., Winterhalter, R., Myhre, C. E. L.,
580 Tsigaridis, K., Vignati, E., Stephanou, E. G., and Wilson, J.: Organic aerosol and global
581 climate modelling: a review, *Atmos. Chem. Phys.*, 5, 1053–1123, 2005.



- 582 Karydis, V. A., Tsimpidi, A. P., Fountoukis, C., Nenes A., Zavala, M., Lei, W., Molina, L. T.,
583 and Pandis, S. N.: Simulating the fine and coarse inorganic particulate matter
584 concentrations in a polluted megacity, *Atmos. Environ.*, 44, 608–620, 2010.
- 585 Koo, B., Knipping, E., and Yarwood, G.: 1.5-Dimensional volatility basis set approach for
586 modeling organic aerosol in CAMx and CMAQ, *Atmos. Environ.*, 95, 158–164, 2014.
- 587 Lipsky, E. M. and Robinson, A. L.: Effects of dilution on fine particle mass and partitioning of
588 semivolatile organics in diesel exhaust and wood smoke, *Environ. Sci. Technol.*, 40, 155–
589 162, 2006.
- 590 Mavko, M.E., and Randall, D.M.: Development of a commodity-based fire emissions tracking
591 system, 17th International Emission Inventory Conference, Portland, OR, available at
592 www.epa.gov/ttn/chief/conferences.html, 2008.
- 593 May, A.A., Levin, E.J. T., Hennigan, C.J., Riipinen, I., Lee, T., Collett, J.L., Jimenez, J.L.,
594 Kreidenweis, S.M., and Robinson, A.L.: Gas-particle partitioning of primary organic
595 aerosol emissions: 3. Biomass burning, *J. Geophys. Res.*, 118, 11327–11338, 2013.
- 596 Murphy, B. N. and Pandis, S. N.: Simulating the formation of semivolatile primary and
597 secondary organic aerosol in a regional chemical transport model, *Environ. Sci. Technol.*,
598 43, 4722–4728, 2009.
- 599 Murphy, B. N., and Pandis, S. N.: Exploring summertime organic aerosol formation in the
600 Eastern United States using a regional-scale budget approach and ambient measurements,
601 *J. Geophys. Res.*, 115, D24216, doi:10.1029/2010JD 014418, 2010.
- 602 NCAR: ARW Version 3 modeling system user’s guide. Prepared by the National Center for
603 Atmospheric Research (NCAR), Boulder, Colorado, 2012.
- 604 NEI TSD: Available at [www.epa.gov/sites/production/files/2015-07/documents/2008_neiv3_](http://www.epa.gov/sites/production/files/2015-07/documents/2008_neiv3_tsd_draft.pdf)
605 [tsd_draft .pdf](http://www.epa.gov/sites/production/files/2015-07/documents/2008_neiv3_tsd_draft.pdf), 2008.
- 606 Pope, C. A.: Respiratory hospital admission associated with PM10 pollution in Utah, Salt Lake
607 and Cache Valleys, *Arch. Environ. Health*, 7, 46–90, 1991.
- 608 Posner, L.N., Theodoritsi, G.N., Robinson, A., Yarwoode, G., Koo, B., Morris, R., Mavko, M.,
609 Moore, T., and Pandis, S.N.: Simulation of fresh and chemically-aged biomass burning
610 organic aerosol, *Atmos. Environ.*, 196, 27–37, 2019.
- 611 Puxbaum, H., Caseiro, A., Sanchez-Ochoa, A., Kasper-Giebl, A., Claeys, M., Gelencser, A.,
612 Legrand, M., Preunkert, S., and Pio, C.: Levoglucosan levels at background sites in



- 613 Europe for assessing the impact of biomass combustion on the aerosol European
614 background, *J. Geophys. Res.* 112, D23S05, doi:10.1029/2006JD008114, 2007.
- 615 Raffuse, S.M., Pryden, D.A., Sullivan, D.C., Larkin, N.K., Strand, T., and Solomon, R.:
616 SMARTFIRE algorithm description. In: Paper Prepared for the U.S. Environmental
617 Protection Agency, Research Triangle Park, NC, by Sonoma Technology, Inc., Petaluma,
618 CA, and the U.S. Forest Service, AirFire Team, Pacific Northwest Research Laboratory,
619 Seattle, WA, STI-905517- 3719, October 2009.
- 620 Roberts, G. C., Andreae, M. O., Zhou, J., and Artaxo, P.: Cloud condensation nuclei in the
621 Amazon Basin: “Marine” conditions over a continent? *Geophys. Res. Lett.*, 28, 2807–
622 2810, 2001.
- 623 Robinson, A. L., Donahue, N. M., Shrivastava, M. K., Weitkamp, E. A., Sage, A. M., Grieshop,
624 A. P., Lane, T. E., Pierce, J. R., and Pandis, S. N.: Rethinking organic aerosol:
625 semivolatile emissions and photochemical aging, *Science*, 315, 1259–1262, 2007.
- 626 Ruminski, M., Kondragunta, S., Draxler, R.R., and Zeng, J.: Recent changes to the hazard
627 mapping system, 15th International Emission Inventory Conference, New Orleans, LA,
628 available at www.epa.gov/ttn/chief/conferences.html, 2006.
- 629 Schwartz, J., Dockery, D. W., and Neas, L. M.: Is daily mortality associated specifically with
630 fine particles? *J. AirWaste Manage.*, 46, 927–939, 1996.
- 631 Seinfeld, J. H. and Pandis, S. N.: *Atmospheric Chemistry and Physics: From Air Pollution to*
632 *Global Change*, second ed., J. Wiley and Sons, New York, USA, 2006.
- 633 Shrivastava, M. K., Lipsky, E. M., Stanier C. O., and Robinson A. L.: Modeling semivolatile
634 organic aerosol mass emissions from combustion systems, *Environ. Sci. Technol.*, 40(8),
635 2671 – 2677, 2006.
- 636 Stanier, C. O., Donahue, N. M., and Pandis, S. N.: Parameterization of secondary organic aerosol
637 mass fraction from smog chamber data, *Atmos. Environ.*, 42, 2276–2299, 2008.
- 638 Theodoritsi, G. N., and Pandis, S. N.: Simulation of the chemical evolution of biomass burning
639 organic aerosol, *Atmos. Chem. Phys.*, 19, 5403–5415, 2019.
- 640 Theodoritsi, G. N., Posner, L. N., Robinson, A., L., Yarwood, G., Koo, B., Morris, R., Mavko,
641 M., Moore, T., and Pandis, S. N.: Biomass burning organic aerosol from prescribed
642 burning and other activities in the United States, *Atmos. Environ.*, in press.



- 643 Tian, D., Wang, Y., Bergin, M., Hu, Y., Liu, Y., and Russell, A.G.: Air quality impacts from
644 prescribed forest fires under different management practices, *Environ. Sci. Technol.*, 42,
645 2767- 2772, 2008.
- 646 Tian, D., Hu, Y., Wang, Y., Boylan, J., W., Zheng, M., and Russell, A. G.: Assessment of
647 Biomass Burning Emissions and Their Impacts on Urban and Regional PM_{2.5}: A
648 Georgia Case Study, *Environ. Sci. Technol.*, 2, 299-305, 2009.
- 649 Tsimpidi, A. P., Karydis, V. A., Zavala, M., Lei, W., Molina, L., Ulbrich, I. M., Jimenez, J. L.,
650 and Pandis, S. N.: Evaluation of the volatility basis-set approach for the simulation of
651 organic aerosol formation in the Mexico City metropolitan area, *Atmos. Chem. Phys.*, 10,
652 525–546, 2010.
- 653 Wang, Z., Hopke P. K., Ahmadi G., Cheng Y. S., and Baron P. A.: Fibrous particle deposition in
654 human nasal passage: The influence of particle length, flow rate, and geometry of nasal
655 airway, *J. Aerosol Sci.*, 39, 1040–1054, 2008.
- 656 Wiedinmyer, C., Quayle, B., Geron, C., Belote, A., McKenzie, D., Zhang, X., O'Neill, S.M., and
657 Wynne, K.: Estimating emissions from fires in North America, *Atmos. Environ.*, 40,
658 3419–3432, 2006.
- 659 WRAP, Western Regional Air Partnership: 2002 Fire emission inventory for the WRAP
660 region—phase II. In: Prepared by Air Sciences, Inc. Project No. 178, July 22, 2005,
661 Available on the Internet at www.wrapair.org/forums/fejftasks/FEJFtask7PhaseII.html,
662 2005.
- 663 WRAP, Western Regional Air Partnership: DEASCO3 2008 emissions inventory methodology.
664 In: Prepared for the Joint Fire Sciences Program, Boise, ID, by Air Sciences Inc., Golden,
665 CO Project No. 178-13, September 2013, Available at wraptools.org/pdf/ei_methodology_20130930.pdf, 2013.
- 667 WRAP, Western Regional Air Partnership: Modifications to the DEASCO3 fire emissions
668 inventory methodology. In: Prepared for the Joint Fire Sciences Program, Boise, ID, by
669 Air Sciences Inc., Golden, CO Project No. 293-1, March 2014.
- 670 Yarwood, G., Rao, S., Yocke, M., and Whitten, G. Z.: Updates to the Carbon bond chemical
671 mechanism: CB05, Prepared by ENVIRON International Corporation, Novato, CA,
672 Yocke & Company, Novato, CA, Smog Reyes, Point Reyes Station, CA, 2005.
- 673



674 **Table 1.** Parameters used to simulate bbPOA, bbSOA-sv and bbSOA-iv in PMCAMx-SR.

675

C^* at 298 K ($\mu\text{g m}^{-3}$)	10^{-1}	10^0	10^1	10^2	10^3	10^4	10^5	10^6
--	-----------	--------	--------	--------	--------	--------	--------	--------

Base Scheme

	Fraction of bbPOA emissions	0.2	0.1	0.1	0.2	0.1	0.3	0.25	0.25
ΔH (kJ mol^{-1})	bbPOA, bbSOA-sv, bbSOA-iv	106	100	94	88	82	76	70	64
MW (g mol^{-1})	bbPOA, bbSOA-sv, bbSOA-iv	250	250	250	250	250	250	250	250

Alternative bbOA scheme

	Fraction of bbPOA emissions	0.2	0.1	0.1	0.2	0.4	0	0	4.75
ΔH (kJ mol^{-1})	bbPOA	-	70	59	48	37	-	-	64
	bbSOA-sv	35	35	35	35	35	35	35	35
	bbSOA-iv	35	35	35	35	35	35	35	35
MW (g mol^{-1})	bbPOA	216	216	216	216	215	215	215	113
	bbSOA-sv	194	189	184	179	179	179	179	179
	bbSOA-iv	149	144	140	135	131	131	131	131

676

677

678

679



680

681 **Table 2.** PMCAMx-SR alternative scheme OA prediction skill metrics against observed values
 682 from STN and IMPROVE networks at biomass-impacted sites.

683

684

685

686

687

688

689

690

691

692

693

694

695

696

697

698

699

700

701

702

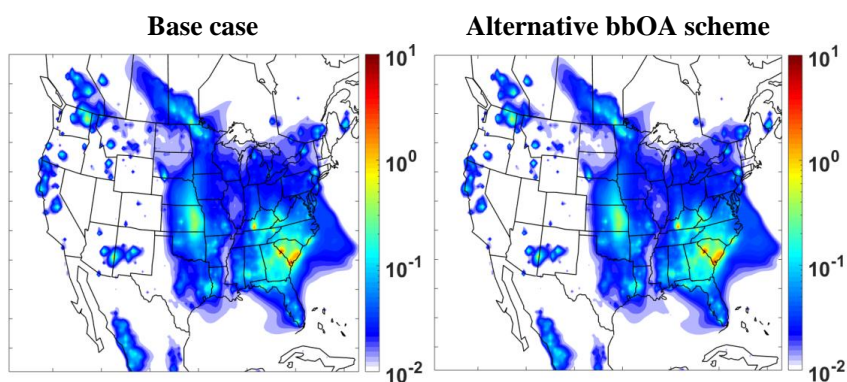
	# Measur.	Mean Observed ($\mu\text{g m}^{-3}$)	Mean Predicted ($\mu\text{g m}^{-3}$)	MB ($\mu\text{g m}^{-3}$)	MAGE ($\mu\text{g m}^{-3}$)	FBIAS	FERROR
bbOA > 0.1 $\mu\text{g m}^{-3}$							
April	538	4.51	4.7	0.19	2.18	0.11	0.48
July	1168	5.14	11.78	6.64	7.72	0.59	0.75
September	937	3.45	6.61	3.16	4.44	0.60	0.77
bbOA > 0.5 $\mu\text{g m}^{-3}$							
April	163	6.29	7.43	1.14	3.07	0.21	0.45
July	468	6.46	20.32	13.85	14.64	0.97	1.01
September	270	4.45	11.90	7.45	9.38	0.85	0.98
bbOA > 1 $\mu\text{g m}^{-3}$							
April	53	7.91	10.22	2.31	4.41	0.28	0.50
July	311	8.20	27.04	18.85	19.86	1.03	1.08
September	150	4.23	16.73	12.50	13.14	1.03	1.10



703

(a) Fresh bbPOA

704

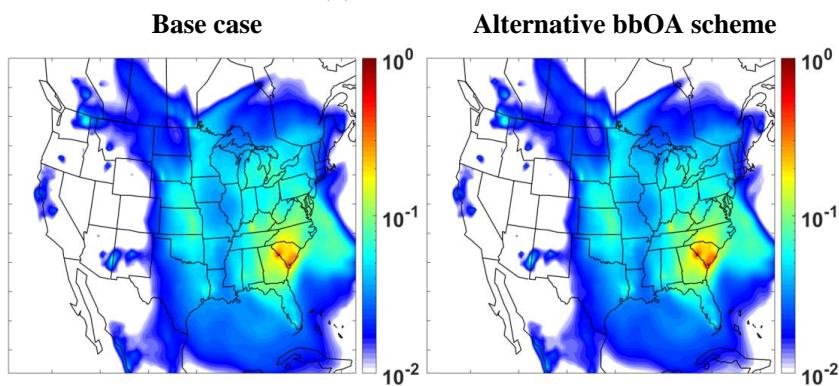


705

706

(b) bbSOA-sv

707

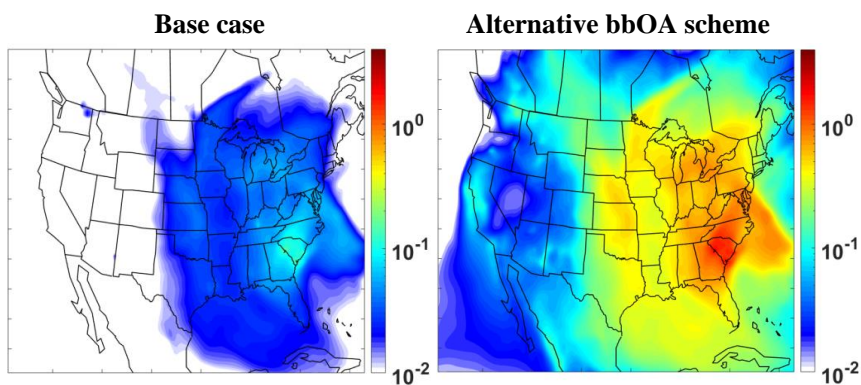


708

709

(c) bbSOA-iv

710



711

712 **Figure 1:** PMCAMx-SR predicted ground – level concentrations of (a) fresh bbPOA, (b) SV-
713 bbSOA-sv and (c) SV-bbSOA-iv from all biomass burning sources during April 2008. Left
714 column refers to the base case simulations and right column to the simulations with the
715 alternative bbOA scheme. All concentrations are in $\mu\text{g m}^{-3}$.



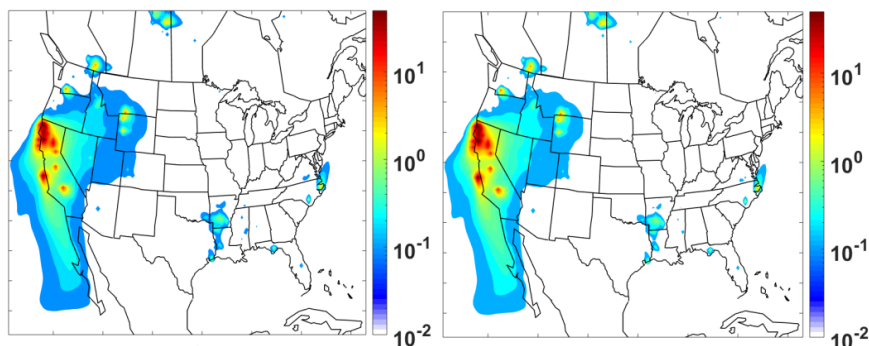
716

(a) Fresh bbPOA

717

Base case

Alternative bbOA scheme



718

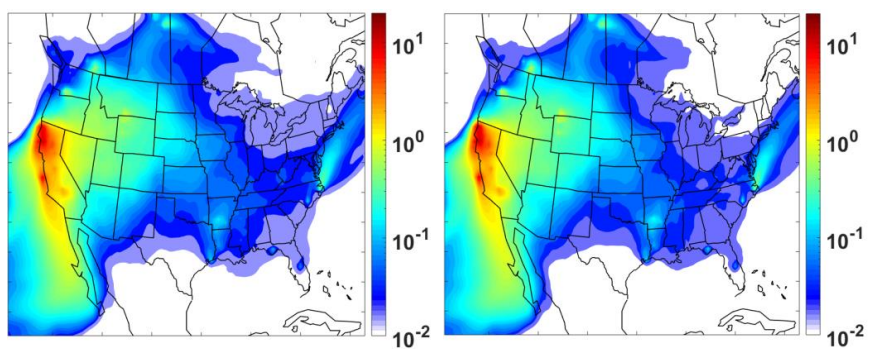
719

(b) bbSOA-sv

720

Base case

Alternative bbOA scheme



721

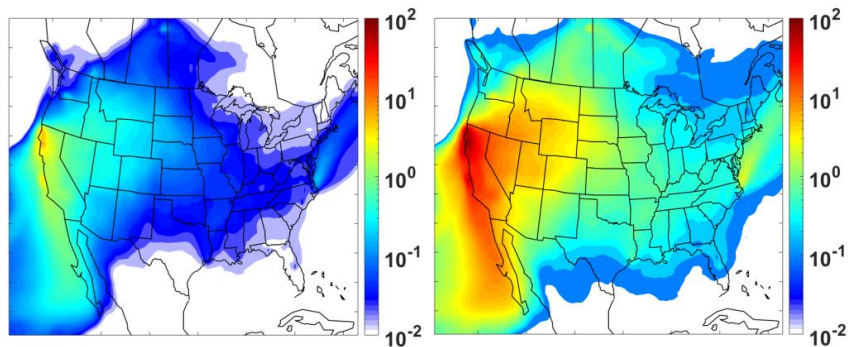
722

(c) bbSOA-iv

723

Base case

Alternative bbOA scheme



724

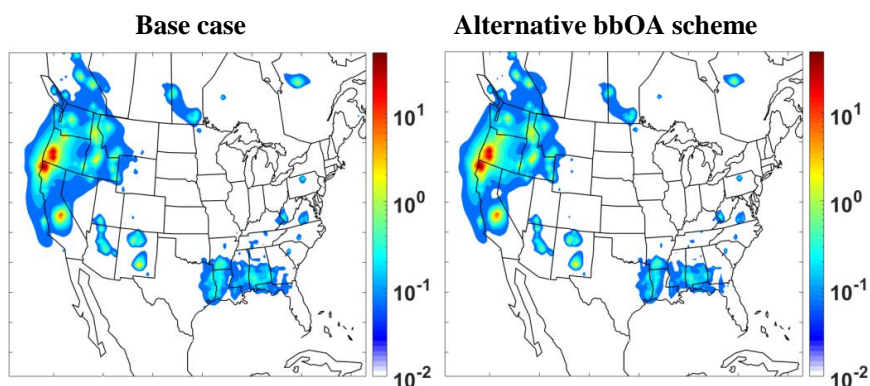
725 **Figure 2:** PMCAMx-SR predicted ground – level concentrations of (a) fresh bbPOA, (b) SV-
726 bbSOA-sv and (c) SV-bbSOA-iv from all biomass burning sources during July 2008. Left
727 column refers to the base case simulations and right column to the simulations with the
728 alternative bbOA scheme. All concentrations are in $\mu\text{g m}^{-3}$.



729

(a) Fresh bbPOA

730

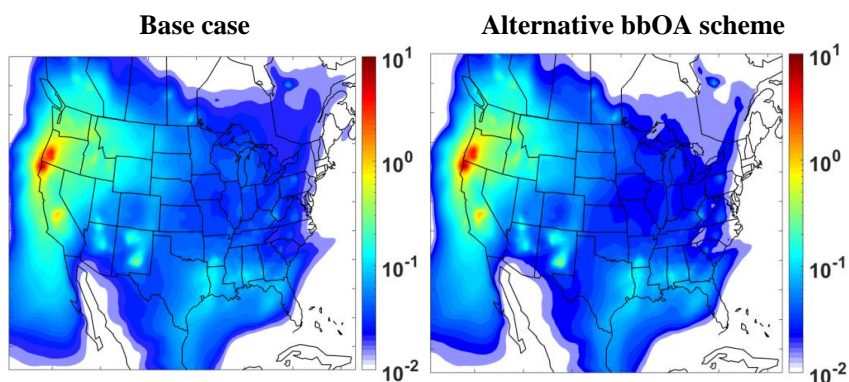


731

732

(b) bbSOA-sv

733

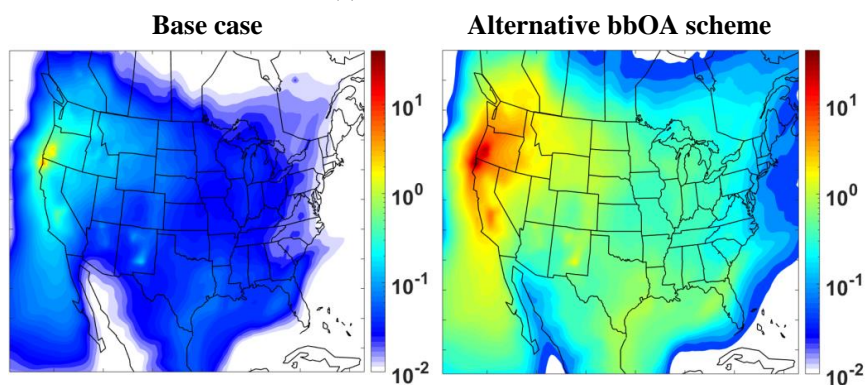


734

735

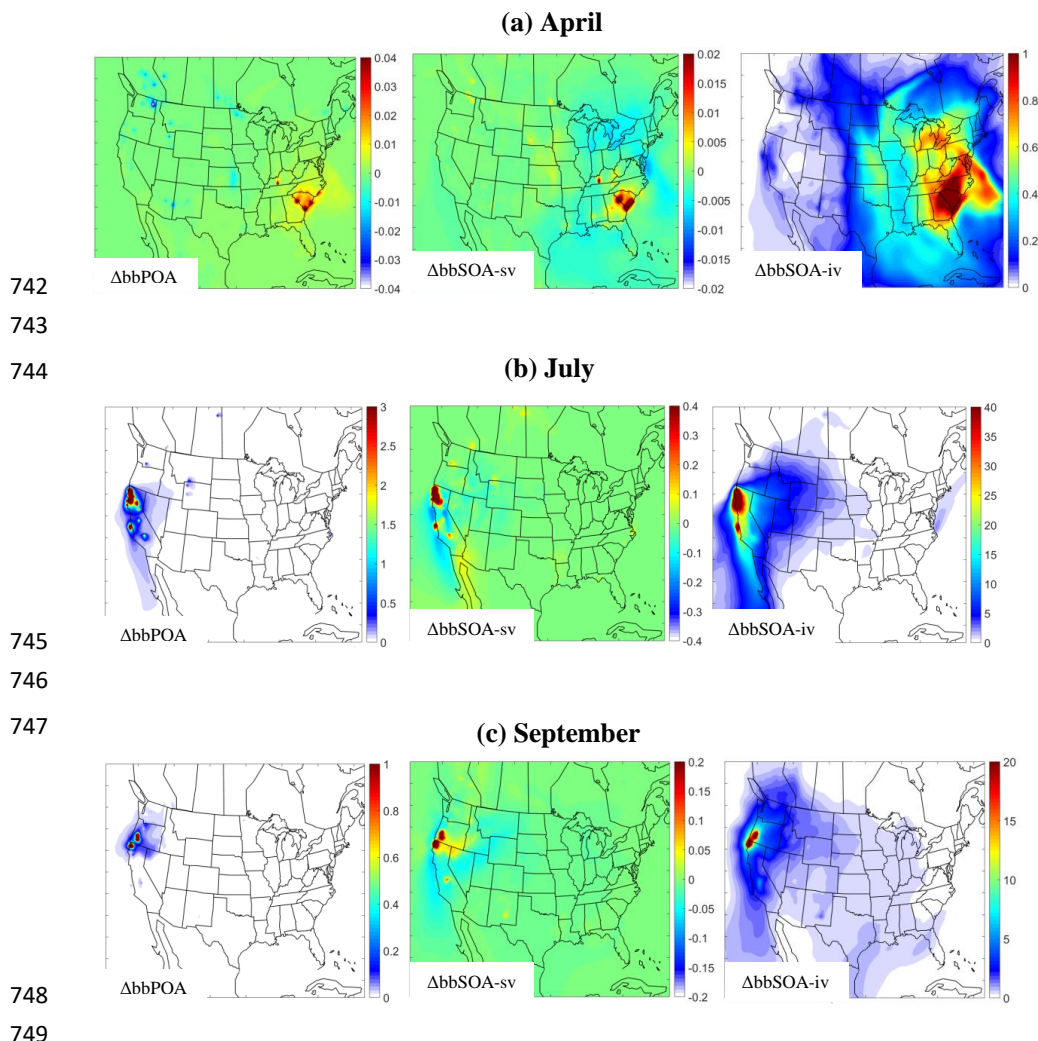
(c) bbSOA-iv

736



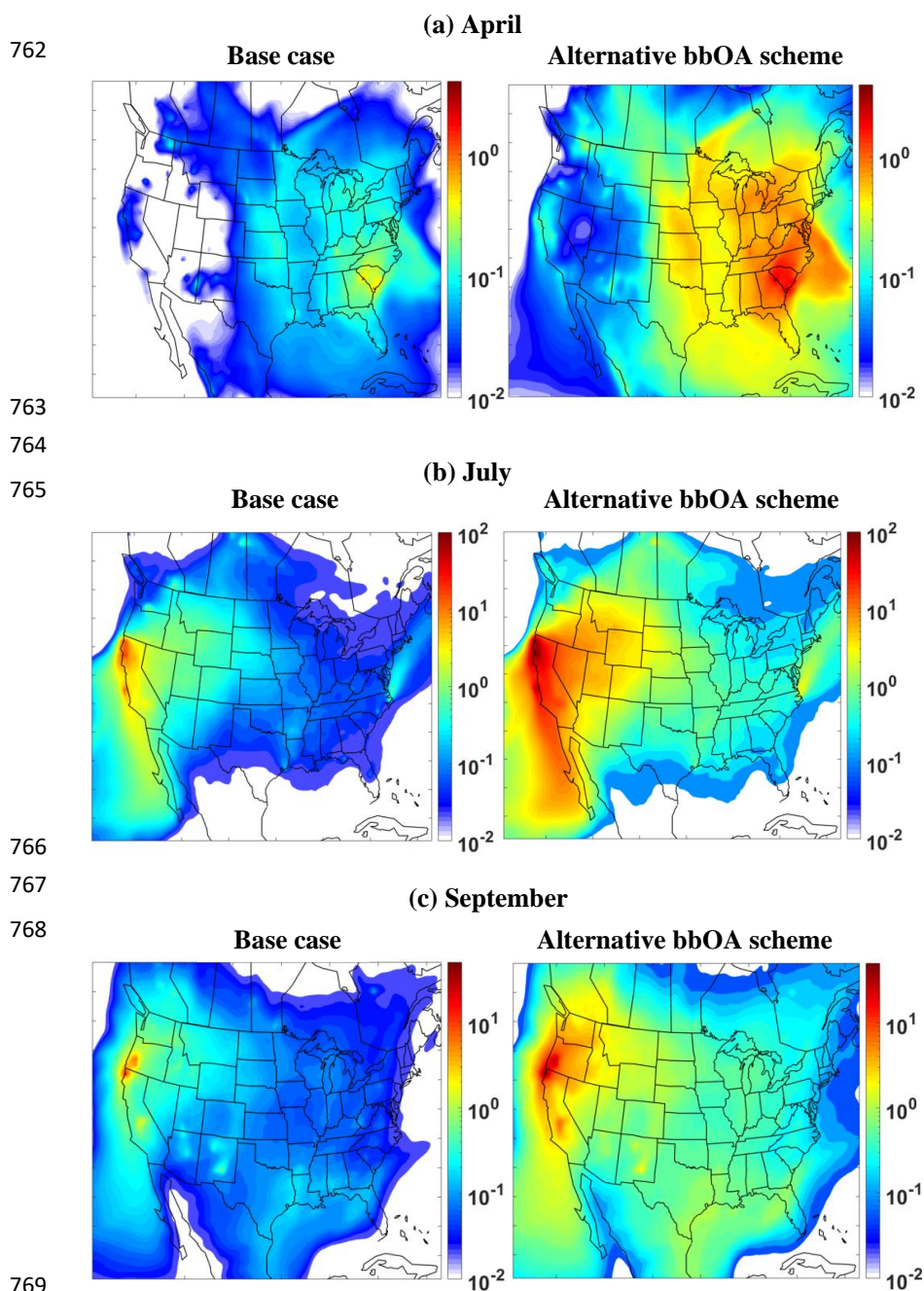
737

738 **Figure 3:** PMCAMx-SR predicted ground – level concentrations of (a) fresh bbPOA, (b) SV-
739 bbSOA-sv and (c) SV-bbSOA-iv from all biomass burning sources during September 2008. Left
740 column refers to the base case simulations and right column to the simulations with the
741 alternative bbOA scheme. All concentrations are in $\mu\text{g m}^{-3}$.



750 **Figure 4:** Average predicted absolute ($\mu\text{g m}^{-3}$) difference (alternative aging scheme minus base
751 case) of ground-level $\text{PM}_{2.5}$ bbPOA, bbSOA-sv and bbSOA-iv concentrations from PMCAMx-
752 SR base case and alternative aging scheme simulations during the modeled periods. Positive
753 values indicate that the PMCAMx-SR alternative aging scheme simulations predicts higher
754 concentrations.

755
756
757
758
759
760
761

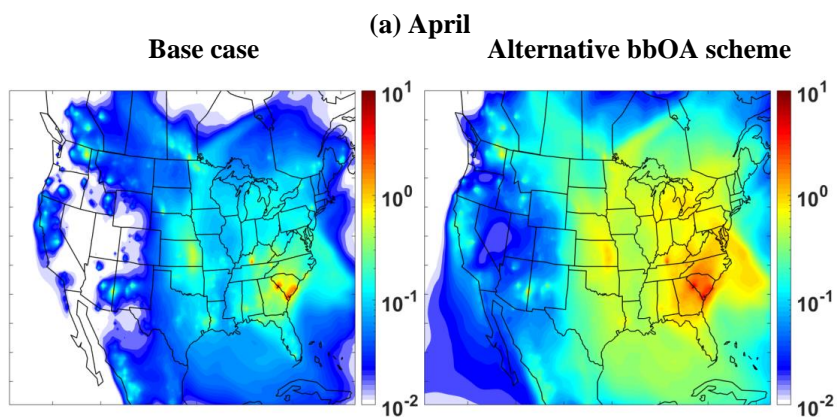


770 **Figure 5:** PMCAMx-SR predicted ground – level concentrations of bbSOA-sv and bbSOA-iv
771 from all biomass burning sources during (a) April, (b) July and (c) September 2008. Left
772 column refers to the base case simulations and right column to the simulations with the
773 alternative bbOA scheme. All concentrations are in $\mu\text{g m}^{-3}$.
774



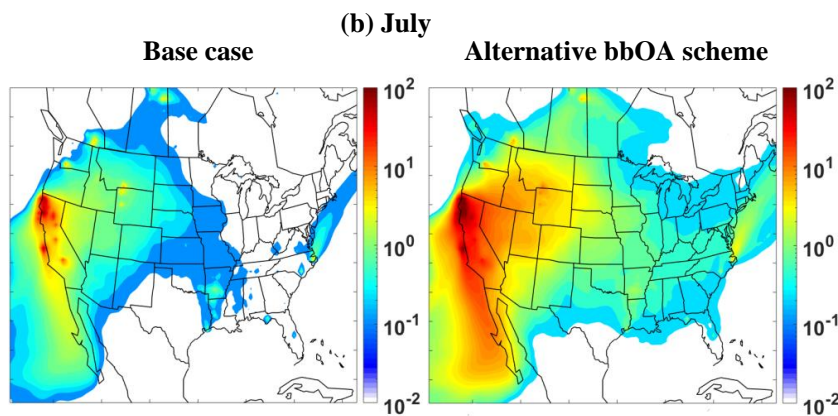
775

776



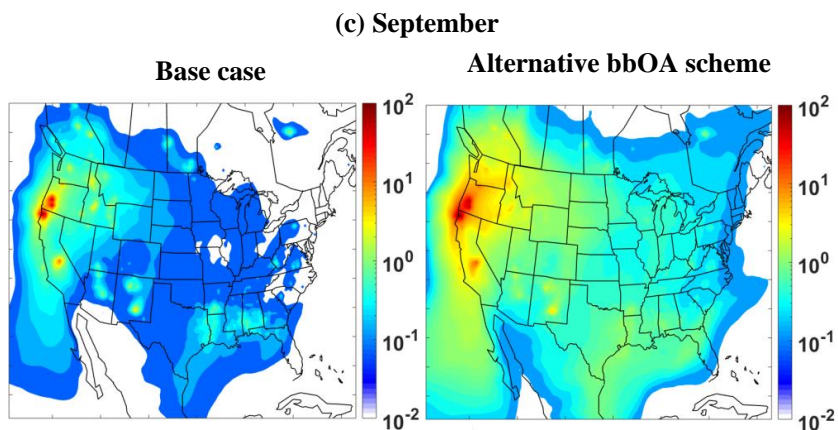
778

779



781

782



784

785

786

787

Figure 6: PMCAMx-SR predicted ground – level concentrations of bbOA from all biomass burning sources during (a) April, (b) July and (c) September 2008. Left column refers to the base case simulations and right column to the simulations with the alternative bbOA scheme. All concentrations are in $\mu\text{g m}^{-3}$.



788

789

790

791

792

793

794

795

796

797

798

799

800

801

802

803

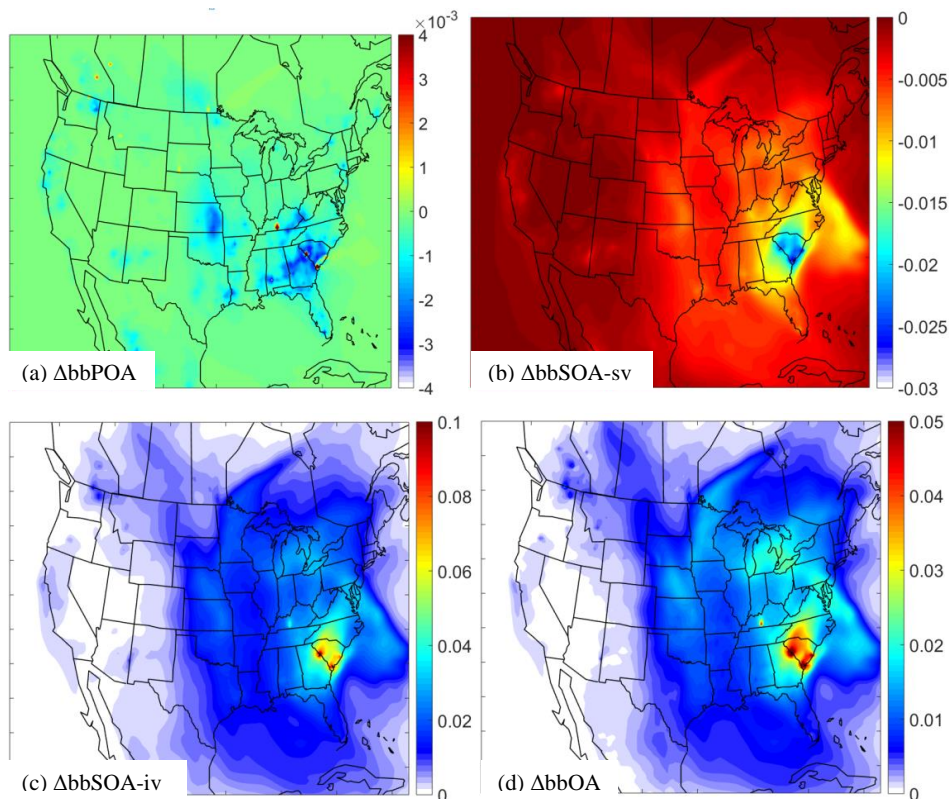


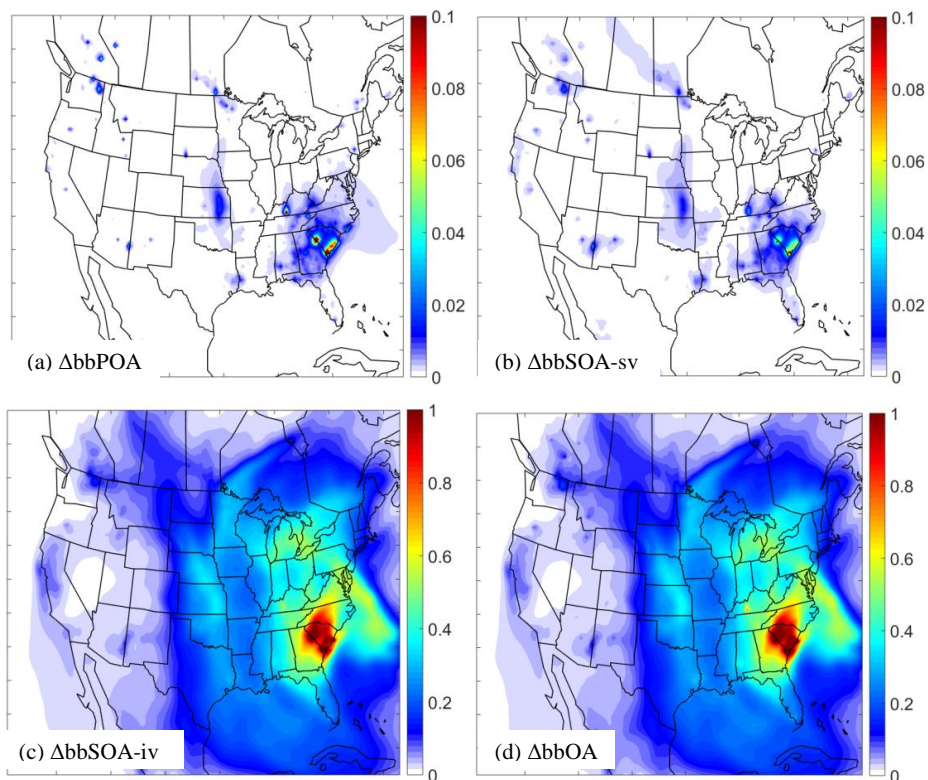
Figure 7: Average predicted increase ($\mu\text{g m}^{-3}$) of the predictions of the base PMCAM_x-SR scheme when the molecular weights and aging stoichiometric coefficient of Ciarelli et al (2017) are used compared to the predictions with the default values for ground-level PM_{2.5} (a) bbPOA, (b) bbSOA-sv (c) bbSOA-iv and (d) bbOA during April 2008. Positive values indicate that the PMCAM_x-SR base scheme with the molecular weights/stoichiometric coefficients of Ciarelli et al. (2017) predicts higher concentrations.



804

805

806



807

808

809 **Figure 8:** Average predicted increase ($\mu\text{g m}^{-3}$) of the predictions of the base PMCAMx-SR
810 scheme when the volatility distribution Ciarelli et al (2017) is used for the biomass burning
811 emissions compared to the predictions with the default values for ground-level $\text{PM}_{2.5}$ (a) bbPOA,
812 (b) bbSOA-sv (c) bbSOA-iv and (d) bbOA during April 2008. Positive values indicate that the
813 PMCAMx-SR base scheme with the volatility distribution of Ciarelli et al. (2017) predicts higher
814 concentrations.

815

816

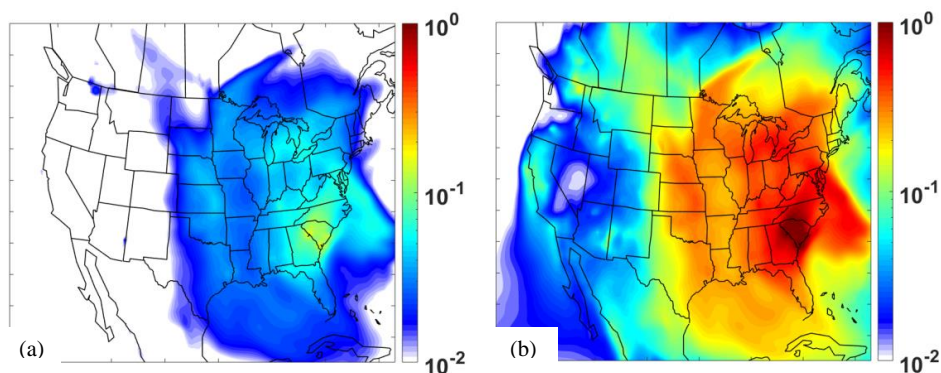
817

818

819



820
821
822
823



824
825
826
827
828
829

Figure 9: PMCAMx-SR predicted ground – level concentrations ($\mu\text{g m}^{-3}$) of bbSOA-iv for the base scheme using (a) the base-case volatility distribution and (b) the Ciarelli et al. (2017) volatility distribution.